Environmental Science & Technology

pubs.acs.org/est

Article

Tire-Derived Transformation Product 6PPD-Quinone Induces Mortality and Transcriptionally Disrupts Vascular Permeability Pathways in Developing Coho Salmon

Justin B. Greer,* Ellie M. Dalsky, Rachael F. Lane, and John D. Hansen

Cite This: *Environ. Sci. Technol.* 2023, 57, 10940−10950

Read Online

ACCESS | Metrics & More | Article Recommendations | Supporting Information

ABSTRACT: Urban stormwater runoff frequently contains the car tire transformation product 6PPD-quinone, which is highly toxic to juvenile and adult coho salmon (*Onchorychus kisutch*). However, it is currently unclear if embryonic stages are impacted. We addressed this by exposing developing coho salmon embryos starting at the eyed stage to three concentrations of 6PPD-quinone twice weekly until hatch. Impacts on survival and growth were assessed. Further, whole-transcriptome sequencing was performed on recently hatched alevin to address the potential mechanism of 6PPD-quinone-induced toxicity. Acute mortality was not elicited in developing coho salmon embryos at environmentally measured concentrations lethal to juveniles and adults, however, growth was inhibited. Immediately after hatching, coho salmon were sensitive to 6PPD-quinone mortality, implicating a large window of juvenile vulnerability prior to smoltification. Molecularly, 6PPD-quinone induced dose-dependent effects that implicated broad dysregulation of genomic pathways governing cell−cell contacts and endothelial permeability. These pathways are consistent with previous observations of macromolecule accumulation in the brains of coho salmon exposed to 6PPD-quinone, implicating blood−brain barrier disruption as a potential pathway for toxicity. Overall, our data suggests that developing coho salmon exposed to 6PPD-quinone are at risk for adverse health events upon hatching while indicating potential mechanism(s) of action for this highly toxic chemical.

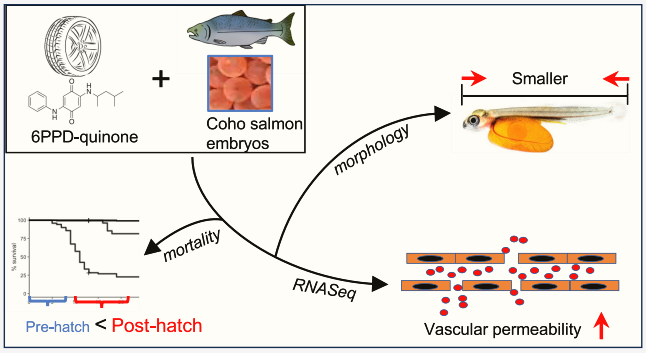

KEYWORDS: *transformation products, urban streams, salmon, nonpoint source pollution*

INTRODUCTION

Populations of coho (*Oncorhynchus kisutch*) and other salmon species on the western coast of the United States and Canada are at historically low abundance, commonly attributed to climate change, freshwater habitat degradation, and fishing pressure.[1−5] Four reproductively isolated populations of coho salmon are currently listed as endangered (Central California Coast) or threatened (Lower Columbia River, Oregon Coast, S Oregon, and N California Coast) under the Endangered Species Act. In highly urbanized watersheds surrounding Seattle, Washington, coho salmon population declines have been linked to acute prespawn mortality induced by toxic stormwater runoff as coho traverse urban waterways to the spawning grounds.[6,7] During the fall run, upward of 90% of female coho salmon succumb to mortality prior to spawning, posing substantial threat of local extinctions of populations residing in urbanized watersheds.[6,8]

While nonpoint source stormwater runoff and traffic density have long been implicated in coho salmon prespawn mortality in urban streams, the toxic chemical responsible for acute prespawn mortality was only recently identified as *N*-(1,3-dimethylbutyl)-*N*′-phenyl-*p*-phenylenediamine-quinone (6PPD-quinone).[9] 6PPD-quinone is an ozonated transformation product of 6PPD, the most abundant substituted *p*-phenylenediamine (PPD) antioxidant added to rubber tires to prevent oxidation and extend service life.[10] The ubiquity of 6PPD in car tires suggests that *p*-phenylenediamine and its transformation products are pervasive globally in urbanized watersheds, and since initial identification of 6PPD-quinone in late 2020, it has been detected in receiving waters and runoff in the United States, Canada, Germany, China, and Australia[11−14] at concentrations up to 2.4 μg/L. Concentrations acutely lethal to coho salmon (LC_{50}: 95 ng/L)[15] occur regularly and can be detected for more than 24 h during rain events.[11,16] Further, at least five different quinone-based transformation products of *p*-phenylenediamine antioxidants have now been identified and

Received: February 8, 2023
Revised: May 25, 2023
Accepted: June 23, 2023
Published: July 19, 2023

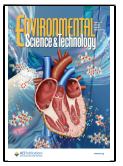

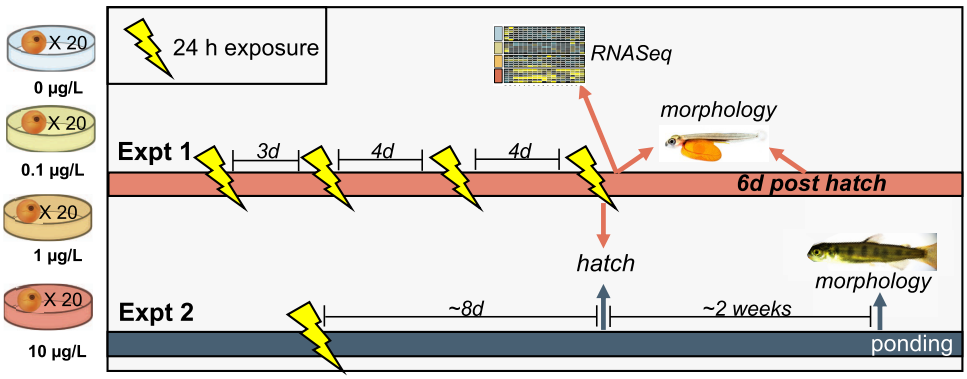

Figure 1. Experimental design for exposure studies. During experiment 1, coho salmon embryos were exposed to three concentrations of 6PPD-quinone (0.1, 1, 10 μg/L nominal) in 24 h pulse exposures twice weekly until hatching. During experiment 2, embryos were exposed to a single 24 h pulse. Greater than 98% of embryos hatched at the indicated hatching date, which occurred during the fourth exposure of experiment 1. Mortality and hatching success were monitored daily throughout both experiments. Morphological assessment included eye area and total length (experiment 1) or fork length (experiment 2).

are likely ubiquitous in urban watersheds,[17] with unknown potential for animal toxicity. Detections of PPDs in airborne particles and dust also raise concern for terrestrial organisms including humans via inhalation, ingestion, and physical contact,[18−20] and recently both 6PPD and 6PPD-quinone have been detected in human urine samples in South China.[21]

Adult and juvenile coho salmon exposed to stormwater containing 6PPD-quinone undergo a common progression of behavioral symptoms termed urban runoff mortality syndrome (URMS) that begins with increased surface swimming, followed by loss of equilibrium and buoyancy, and eventual death.[22,23] After the onset of symptoms fish do not recover when transferred to clean water.[22,24] Blood chemistry in symptomatic fish has demonstrated increased hematocrit and plasma leakage from the cerebrovasculature, suggesting loss of integrity of cell−cell adhesions in the blood−brain barrier (BBB) and endothelial junctions.[25]

Given the recent identification of 6PPD-quinone, few studies to date have assessed its effects on other fish species but have demonstrated a wide range of sensitivity. Brook trout (*Salvelinus fontinalis*) and rainbow trout (*Oncorhynchus mykiss*) are 6- to 10-fold less sensitive than coho salmon but still exhibit mortality at environmentally measured concentrations,[26] while several other species (Chinook salmon (*O. tshawytscha*), sockey salmon (*O. nerka*), zebrafish (*Danio rerio*), white sturgeon (*Acepenser transmontanus*), arctic char (*Salvelinus alpinus*), Japanese medaka (*Oryzias latipes*), Atlantic salmon (*Salmo salar*), brown trout (*Salmo trutta*)) do not show behavioral symptoms or reduced survivorship at concentrations likely to be encountered in the environment.[23,26−29] Insights into the mechanism of action of 6PDD-quinone will provide critical information to better understand the broad range of observed species sensitivity. With reductions in recruitment capacity of up to 90% in urban watersheds due to adult prespawn mortality, impacts on annual recruitment could further accelerate coho salmon population declines. We therefore investigated the effects of 6PPD-quinone on developing coho salmon embryos using survival studies coupled with morphology and transcriptomic assessments.

Coho salmon embryos were exposed to 6PPD-quinone using twice weekly 24 h pulse exposures to mimic intermittent rainfall events common during the fall coho spawning season in the Pacific Northwest (PNW). We documented significant effects on survivorship and growth with as little as one 24 h pulse of 6PPD-quinone at environmentally observed concentrations. Further, we provide the first assessment of global transcriptomic responses in coho salmon to 6PPD-quinone in an effort to explore the mechanism of toxicity. Strong dose-dependent effects were observed relating to developmental pathways, including skeletal muscle development, blood vessel formation, and ossification. Pathways and molecules innervating endothelial cell−cell adhesion, hemostasis, and blood coagulation were perturbed at all concentrations and provided molecular linkages to observed blood−brain barrier disruptions. Our findings suggest that in addition to adult prespawn mortality, 6PDD-quinone induces reductions in survival and fitness of progeny that represent a substantial concern for urban spawning coho salmon populations.

MATERIALS AND METHODS

Chemicals. 6PPD-quinone, the internal standard 6PPD-quinone-D5, and analytical independent check standard 6PPD-quinone were obtained from HPC Standards (purity 97.26%). All other chemicals were from Millipore Sigma and Fisher Scientific.

Embryo Rearing. Fertilized coho salmon embryos at the eyed egg stage were obtained from two fish hatcheries: the Issaquah Salmon Hatchery in Issaquah, WA, and Yakima Nation Fisheries Hatchery Complex in Yakima, WA. Eggs were transported to the U.S. Geological Survey Western Fisheries Research Center in Seattle, WA, and reared in egg stacks with spinning disc filtered (2 μM final) and ultraviolet (UV)-treated fresh water from Lake Washington (100 μS) maintained at 8.0−8.5 °C. Embryos were acclimated for a minimum of 96 h before initial exposure. All experimental protocols were approved by the Animal Care and Use Committee at the U.S. Geological Survey Western Fisheries Research Center (Protocol #2008-73).

6PPD-Quinone Exposures. Static 24 h exposures to nominal 6PPD-quinone concentrations of 0.1, 1, or 10 μg/L or a DMSO solvent carrier control were carried out in glass Petri dishes (150 mm × 20 mm) containing 170 mL of water at a density of 20 embryos per dish. Each exposure period covered eight accumulated temperature units (ATUs) of embryonic development. Embryos were carefully transferred from the egg stacks to exposure dishes using a slotted spoon for each exposure. Dishes were placed at the bottom of circular 2 ft.

https://doi.org/10.1021/acs.est.3c01040
Environ. Sci. Technol. 2023, 57, 10940−10950

tanks and surrounded by low-flow temperature-controlled water to maintain 8.5 °C in exposure dishes. Each tank contained two dishes per concentration to minimize potential tank effects. A working 1× stock solution of 10 μg/L 6PPD-quinone in process water was prepared immediately prior to the start of exposure and serial diluted to obtain 1× working solutions of 1.0 and 0.1 μg/L.

For experiment 1, embryos obtained from the Issaquah Salmon Hatchery (Issaquah, WA) were exposed to 6PPD-quinone or solvent carrier control twice per week until hatch (6 replicate dishes, n = 120 embryos/concentration) to mimic intermittent winter rain events. After each 24 h exposure, eggs were carefully transferred back to egg rearing trays (1 tray per treatment group) and maintained in clean flowing water. Embryos that hatched prior to the final exposure were excluded from subsequent exposures but continued to be monitored for mortality. Surviving, unhatched embryos were randomly distributed to the dishes for the next exposure. In the event of mortalities, fewer dishes were used but were maintained at 20 embryos/dish for density consistency. In experiment 2, a single 24 h exposure was performed similarly as described above on eyed eggs obtained from the Yakima Nation Fisheries Hatchery Complex (Toppenish, WA). A full schematic of exposure regimes and endpoints for each experiment can be found in Figure 1A.

Mortality, Hatching Success, and Phenotypic Measurements. Mortality and hatching were monitored daily throughout each experiment, with hatching defined as the complete liberation of both the head and tail from the chorion. Embryos exhibiting abnormal phenotypes were monitored for a minimum of 24 h to ensure the embryo was not in the process of a successful hatch. Measurements of growth and development were assessed at two time points from experiment 1 and one time point from experiment 2 (Figure 1A). Larvae assessed in experiment 1 were collected directly from the glass exposure dishes following the fourth exposure in which most embryos hatched to ensure that all larvae measured were less than 24 h posthatch. For both experiments, larvae were randomly selected from each treatment, euthanized in Tricaine-S (MS-222), and immediately stored in formalin fixative. Larvae were transferred to 70% ethanol prior to imaging. Images were taken using a Keyence BZX-710 fluorescent microscope at 2× magnification. Due to the large size of the larvae, the image merge function was used to stitch images together into one measurable image. Standard length was measured from experiment 1 larvae, and fork length was measured from Experiment 2 larvae due to their larger size. Eye area was also assessed using Keyence analysis software using the XY measurement and area measurement features. Visualization of the heart and surrounding cardiac tissue was obscured by the yolk sac, and therefore, pericardial edema could not be measured.

Concentrations of 6PPD-Quinone Determined by Liquid Chromatography-Mass Spectrometry. Exposure samples were collected in 4 mL amber glass vials and stored at −20 °C until analysis. Samples from experiment 1 were collected in duplicate: 6PPD-quinone initial and final concentrations were assessed from the second and fourth exposures and the initial concentration from the third exposure. For experiment 2, triplicate water samples were assessed at six time points over the 24 h exposure. Concentrations of 6PPD-quinone were determined by direct injection ultraperformance liquid chromatography/tandem mass spectrometry (UPLC/MS/MS). The method used an isotope dilution approach with the isotopically labeled surrogate internal standard 6PPD-quinone-D5 and had a 0.002 μg/L reporting limit. Chromatographic separation was achieved with an Acquity H-Class Bio UPLC (Waters Corporation) equipped with an Acquity UPLC BEH C18, 1.7 μm 2.1 mm × 50 mm column and corresponding guard column held at 40 °C with a 0.5 mL/min flow rate and 0.1% formic acid in water and acetonitrile gradient, and the injection volumes ranged from 1 to 50 μL. For detection, an API 5500 Triple Quadrupole Mass Spectrometer (Sciex LLC) used positive electrospray ionization with multireaction monitoring, and parameters were optimized for the following ion transitions: m/z 299.1 → 215.1 for 6PPD-quinone quantitation, 299.1 → 187.1 for 6PPD-quinone confirmation, and 304.1 → 220.2 for 6PPD-quinone-D5. Identification was based on the retention time and the ratio of the two MRM transitions being within ±25%. For quantification, calibration curves used ≥7 points with concentrations ranging from 0.001 to 20 μg/L and a $1/x$ weighting was applied. The following quality control samples were also analyzed and within acceptance criteria: check and independent check standards ranged from 0.01 to 10 μg/L with an 80−118% accuracy, spike recovery samples were spiked at 0.25 and 11 μg/L and had an 80−88% recovery, instrument replicate injections were within ±20% of each other, laboratory duplicate samples had a 2−18% difference, and 43 laboratory blanks were nondetects.

RNA Extraction and Library Preparation. Transcriptomic effects of exposure were assessed in larvae from experiment 1. Recently hatched (<24 h) larvae were collected from exposure dishes from all three concentrations and the carrier controls at the end of the 24 h period of the fourth exposure (n = 7). Larvae were euthanized in buffered MS-222 and then stored in RNALater (Qiagen). Immediately prior to RNA extractions, larvae were removed from RNALater and the yolk sac was quickly removed with sterile forceps and scissors. Larvae were then transferred to RLT Lysis Buffer (Qiagen) and homogenized with homogenizing beads using an MP Fast Prep 24 homogenizer (MP Biomedicals, Irvine, CA). Total RNA was extracted from whole larvae homogenate with the RNEasy mini kit (Qiagen) following the manufacturer's protocols. Quantity and quality of total RNA for each sample were assessed with an Agilent 2100 Bioanalyzer (Agilent Technologies, Palo Alto, CA) prior to library preparation.

Libraries were prepared from 500 ng of total RNA with the NEBNext Ultra II Direction RNA Library Prep Kit (New England Biolabs, Ipswich, MA) following the manufacturer's protocols, with the NEBNext rRNA depletion kit (Human/Mouse/Rat) used for mRNA enrichment of total RNA. Quantity and fragment size of final complementary cDNA libraries were assessed on the Agilent 2100 Bioanalyzer. Libraries were multiplexed and sequenced as 75 bp single-end reads on 1 lane of a NextSeq. 500 at the University of California Riverside genomics facility (Riverside, CA). One individual from the lowest treatment (0.1 μg/L) was removed due to poor RNA quality, and one sequencing library was unsuccessful from the medium treatment (1 μg/L), resulting in 6 biological replicates for these treatments.

RNASeq Bioinformatic Processing. Quality control and adapter removal of the raw reads were performed with trimmomatic (v0.39)[30] and read quality and sequencing depth were assessed with FastQC.[31] Cleaned reads passing quality control were quantified using the*O. kisutch* tran-

https://doi.org/10.1021/acs.est.3c01040
Environ. Sci. Technol. 2023, 57, 10940−10950

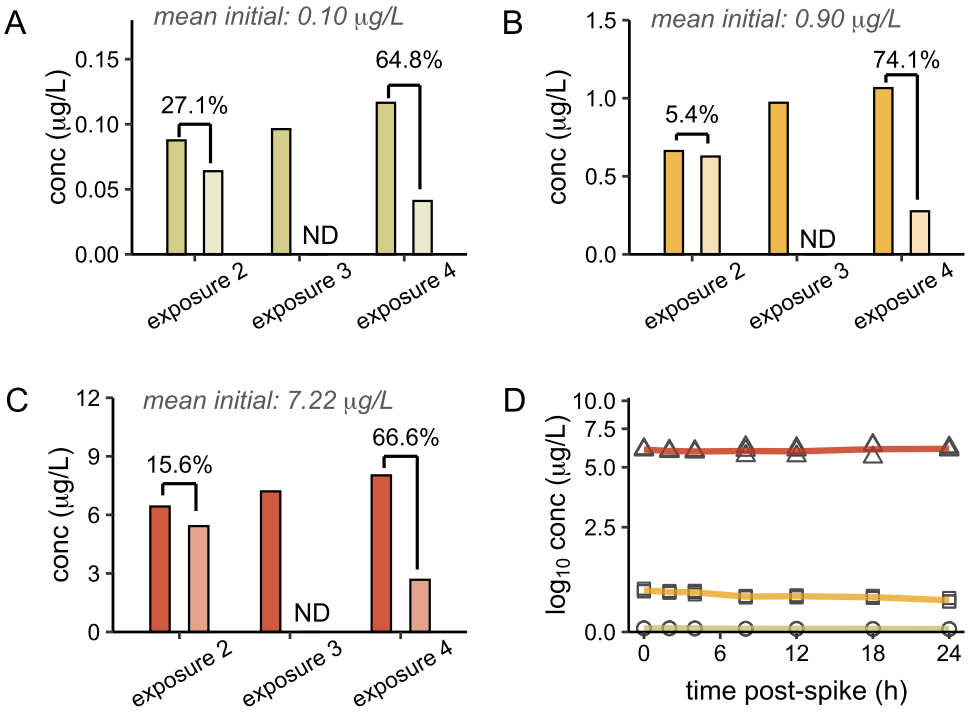

Figure 2. Analytical assessment of 6PPD-quinone concentrations. (A−D) Analysis of 6PPD-quinone concentrations measured in duplicate by UPLC/MS/MS from experiment 1. Dark bars represent measurements at the beginning of the exposure period and light bars indicate measurements at the end of the 24 h exposure. Mean initial exposure concentrations are indicated at the top of each panel for nominal concentrations of 0.1 μg/L (B), 1 μg/L (C), and 10 μg/L (D). Percent loss of the compound during the 24 h period is indicated above each exposure. Measurements were not determined (ND) during exposure 1 or at the end of exposure 3. Percentages indicate the percent loss of 6PPD-quinone during the exposure period. (E) Time course of water chemistry from the single exposure in experiment 2. Each concentration and time point were measured in triplicate.

scriptome and genome obtained from NCBI (refseq accession GCF_002021735.2, retrieved 3/28/2022) using salmon (v1.8.0)[32] in mapping mode with selective alignment. Fragment length mean (fldMean) was set to 415, and fragment length standard deviation (fldSD) was set to 50 based on fragment sizes determined from the bioanalyzer trace of the final pooled library.

Quantification outputs from salmon were imported into R with tximport (v1.16.1), with quantification aggregated from the transcript to the gene level using transcript/gene relationships extracted from the *O. kisutch* feature table obtained from the NCBI. Treatment-induced differential expression was assessed in DeSeq2 (v1.32.0) using a likelihood ratio test[33] with statistical significance defined as $p \leq 0.05$, following Benjamini-Hochberg (BH) false discovery rate correction. Differentially expressed transcripts were clustered with DIANA hierarchical clustering using degPatterns in the DEGreport package[34] with reduce = T and a minimum of 10 genes per cluster to evaluate clusters of differentially expressed transcripts with similar expression patterns across treatments. Heatmaps were created using the ComplexHeatmap package in R.[35]

Pathway analysis was assessed on clusters of differentially expressed genes using the clusterProfiler package in R.[36] A large proportion of genes from the *O. kisutch* genome lacked gene symbols necessary for pathway analysis. Therefore, prior to analysis, we linked the NCBI gene IDs with the better-annotated ENSEMBL gene IDs extracted from the ENSEMBL transcriptome FASTA file. Further gene annotations for genes still without a gene symbol were performed by matching the gene name to its *Homo sapien* counterpart in the org.Hs.eg.db database in R.

Statistical Analysis. Statistical significance for mortality and timing of hatch was assessed by Kaplan−Meier analysis implemented with the *drc* package in R. For length (total length for experiment 1 and fork length for experiment 2) and eye area, normality of the data was assessed with a Shapiro-Wilk test. Statistical significance was assessed with a one-way analysis of variance (ANOVA) and Tukey's post-hoc test for normally distributed data. For non-normally distributed data, statistical significance was assessed using a Kruskal−Wallis one-way ANOVA, followed by Dunn's post-hoc testing.

RESULTS AND DISCUSSION

Identification of 6PPD-quinone as the causative stormwater toxicant of coho salmon URMS shed light on over two decades of mass prespawn mortality events in urban streams of the PNW. The intense ecological risk posed to coho salmon populations traversing urban regions is the consequence of several biological and ecological factors. First, coho salmon are acutely sensitive to 6PPD-quinone at very low concentrations, making it one of the most toxic aquatic chemicals described compared to other toxicants with EPA-established aquatic life criteria.[15] Second, the fall freshwater spawning migration is triggered by the onset of the autumn rainfall when contaminant levels from stormwater runoff are frequently at their highest levels.[37] Individuals that successfully spawn commonly do so in shallow, low-lying streams where elevated levels of stormwater contaminants can persist for hours or days with high peak contaminant concentrations.[37]

https://doi.org/10.1021/acs.est.3c01040
Environ. Sci. Technol. 2023, 57, 10940−10950

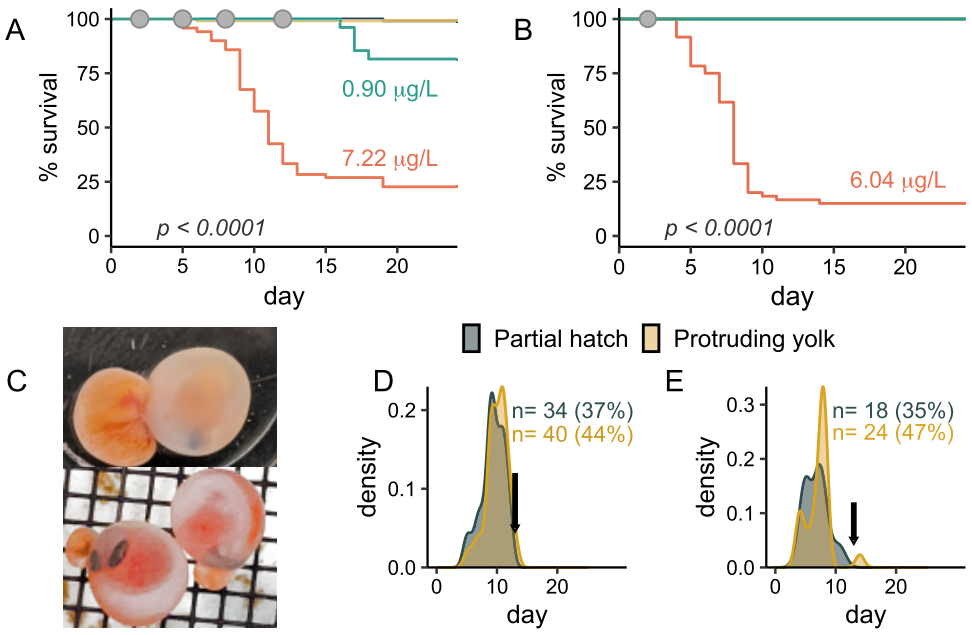

Figure 3. Mortality and associated phenotypes. (A) Kaplan−Meier survival analysis from experiment 1 (n = 120). Gray dots indicate 24 h periods of 6PPD-quinone exposure. X-axis represents days post 6PPD-quinone exposure, with the first exposure occurring on day 2 (372 ATUs). Significant mortality was induced at 0.90 and 7.22 μg/L (log-rank test, BH correction). Embryonic mortality was not observed at 0.95 μg/L (yellow line). (B) Kaplan−Meier survival analysis from experiment 2 (n = 60), with gray dot indicating the timing of exposure. X-axis represents days post 6PPD-quinone exposure, with the first exposure occurring on day 2 (390 ATUs). Significant mortality was induced after one exposure to 6.04 μg/L (log-rank test) (C) Representative gross morphology of embryos with protrusion of the yolk sac (orange) from the chorion, a phenotype that was fatal. (D) Density plot indicating timing of protruding yolk sac and partial hatching phenotypes from the high exposure concentration for experiment 1 (left panel) and experiment 2 (right panel). N represents the total number of mortalities, percentage indicates the proportion of total mortalities, and arrows indicate the hatching date for healthy individuals.

Embryonic Exposure to 6PPD-Quinone Induces Mortality and May Bioaccumulate in Hatched Alevin. We first investigated the potential for environmentally observed concentrations of 6PPD-quinone to elicit acute mortality using 24 h pulse exposures twice per week until hatch (n = 120 embryos/treatment) to mimic intermittent rain events that produce high volumes of stormwater runoff during the fall and winter in the Pacific Northwest. A total of four pulse exposures were performed (Figure 1), with mean initial exposure concentrations of 0.10, 0.90, and 7.22 μg/L (Figure 2A−C). Significant embryonic mortality was observed at 7.22 μg/L in experiment 1 (log-rank test, $p < 0.001$) beginning at the onset of the second exposure, and only 21% of those embryos survived through hatching and yolk sac internalization (Figure 3A). Further, this acute toxicity was observed at later embryonic stages following eye pigmentation (>370 ATUs, 52 days postfertilization) that is typically considered less sensitive than earlier embryonic stages.[38]

We then repeated the experiment to assess if a single 24 h exposure was sufficient to induce mortality (n = 60). Significant mortality was induced at 6.04 μg/L (log-rank test, $p < 0.01$, Figure 3B), with embryos dying at a rate of ∼10 per day until hatching. Overall survival was lower than in experiment 1, and time to mortality was significantly shorter ($p \leq 0.05$) despite receiving only a single 24 h pulse of 6PPD-quinone.

The chorion that surrounds developing fish embryos provides a physical barrier that can restrict compound uptake and reduce toxicity to some chemicals[39] and likely contributed to greater than 99% survival at 0.10 μg/L, the estimated 24 h LC50 in juvenile coho salmon[9,15] (Figure 3A,B). Predictions of 6PPD-quinone chorion permeability are difficult to address due to the large number of physical and chemical properties that affect substance permeability,[40−42] however, during experiment 1, recovery of 72% or greater for 6PPD-quinone at the end of the second exposure indicated that uptake was likely minimal during these exposure periods (Figure 2A−C). Similar stability of 6PPD-quinone was observed during single pulse exposures in experiment 2, lending support to minimal absorption of 6PPD-quinone during embryonic stages (Figure 2D). Conversely, during the fourth exposure in experiment 1, greater than 98% of exposed embryos from each treatment unexpectedly hatched overnight and were directly exposed to 6PPD-quinone for ∼6−12 h. Compound recovery at the end of this exposure was substantially lower across all concentrations (25.9−35.2%), suggesting active uptake or absorption occurred immediately after hatching. This brief exposure of alevin to 6PPD-quinone did not elicit immediate mortality, however, 17% of fish exposed to 0.90 μg/L exhibited significant delayed mortality over a three-day period beginning 5 days after hatch (log-rank test, BH correction, $p < 0.001$, Figure 3A). No mortality occurred at 0.95 μg/L. All remaining individuals from the 7.22 μg/L concentration were collected for molecular and morphological endpoints, and mortality was no longer monitored.

An inability of juvenile fish to recover after the onset of symptoms[22,24] and our observations of delayed mortality postexposure implicate slow elimination of 6PPD-quinone in coho alevin. Rapid uptake posthatch and slow elimination commonly lead to bioaccumulation. 6PPD is expected to be highly bioaccumulative,[43] and 6PPD-quinone and its suspected monohydroxylated metabolite can be detected in the brain and gills immediately after exposure that suggest compound

https://doi.org/10.1021/acs.est.3c01040
Environ. Sci. Technol. 2023, 57, 10940−10950

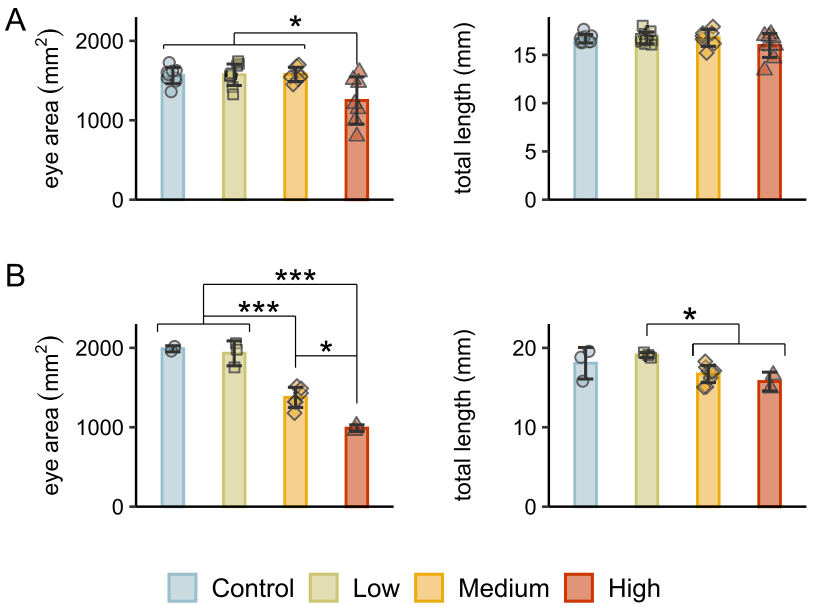

Figure 4. Altered development in surviving alevin in experiment 1. (A) Total fish length was significantly reduced at 7.22 μg/L immediately after hatching ($p < 0.05$, Kruskal–Wallace test, Dunn's post-hoc, $n = 10$), but eye area was unaffected. (B) Total length and eye area were both significantly reduced at high concentrations in alevin at 6 days posthatch ($p < 0.05$, ANOVA, Tukey's post-hoc).

uptake.[29] The duration of tissue persistence, however, is unclear.

Such future studies are highly relevant for risk assessments in the PNW, where low freshwater survival rates of out-migrating smolt are a significant contributor to coho salmon population declines,[44] and fry can spend a year or more in the watershed prior to ocean migration and encounter multiple stormwater pollution events.

Embryonic mortalities were commonly observed (>80%) as one of two distinct phenotypes: either protrusion of the yolk sac from the chorion, typically near the head (Figure 3C), or partial hatching of only the head that never progressed to full hatch. Each phenotype occurred well in advance of the expected hatching day and thus may be indicative of early induction of hatching prior to full embryonic development. In support of this hypothesis, we observed a trend of earlier onset of hatching at all three concentrations during experiment 1, with 10–15% of embryos hatching prior to the primary hatching day compared to 5% for controls. Early hatching was lethal, as no fish hatching >5 days prior to the common hatching date survived through yolk sac internalization. We were unable to find any literature describing similar phenotypes in salmonid embryos, and therefore, this may represent a unique toxicity outcome for 6PPD-quinone.

Impaired Growth and Development of Surviving Embryos. After observing the earlier onset of hatching in experiment 1 and mortalities that appeared to be related to premature hatching, we then examined surviving alevin for morphological signs of altered development. Immediately after hatching in experiment 1, alevin exposed to 7.22 μg/L showed significantly reduced eye area compared to all other treatments (Figure 4A). At 6 days posthatch (dph), significant reductions were noted for eye area and total length for both 0.90 and 7.22 μg/L concentrations (Figure 4B). There were no effects on morphology at the timing of yolk sac internalization after the single exposure for experiment 2. Other gross malformations including lordosis and yolk sac edema were not observed.

Dose-Dependent Effects of 6PPD-Quinone on Global Transcriptomic Patterns. Substantial species-dependent toxicity, especially within *Oncorhynchus* and *Salvelinus*, highlights a critical need for investigations into the mechanism of action for 6PPD-quinone. The most closely related species to coho salmon (Chinook salmon, chum salmon(*O. keta*), and sockeye salmon) are relatively insensitive to 6PPD-quinone mortality,[23,24,45] while in some more distantly related species (rainbow trout, brook trout, and white-spotted char), mortality is induced at concentrations less than 1 μg/L.[26,29] 6PPD and 6PPD-quinone are also detected in human urine samples, with further elevated levels in pregnant women.[21] Thus, the mechanism of 6PPD-quinone toxicity also has important implications for human health and terrestrial organisms as a whole.

We performed whole-transcriptome sequencing on alevin that hatched during the fourth exposure in experiment 1 to better understand the molecular basis for 6PPD-quinone-induced mortality and developmental abnormalities ($n = 6–7$/treatment). A likelihood ratio test identified 1886 differentially expressed genes (DEGs, $p_{adj} \leq 0.05$, Table S1) across all concentrations compared to controls out of a total of 29,278 genes with measurable expression. Hierarchical clustering of DEGs categorized 1822 of the DEGs into seven distinct transcriptional patterns, each of which demonstrated a dose-dependent effect of 6PPD-quinone (Figure 5).

BBB permeability is governed by tight junctions (TJs) and adherens junctions (AJs) that regulate contacts between adjacent endothelial cells to form the principal barrier restricting polar macromolecule diffusion into the central nervous system. Integrity of the BBB is critical for central nervous system function, and BBB disruptions are associated with trauma, hemorrhagic stroke, and inflammation and can lead to neuronal dysfunction, brain edema, paralysis, and death.[46–48] Coho displaying stormwater-induced UMRS display hemoconcentration and macromolecule accumulation in cerebral tissues that signify disruption of junctional complexes,[25] introduction of paracellular gaps, and loss of

https://doi.org/10.1021/acs.est.3c01040
Environ. Sci. Technol. 2023, 57, 10940–10950

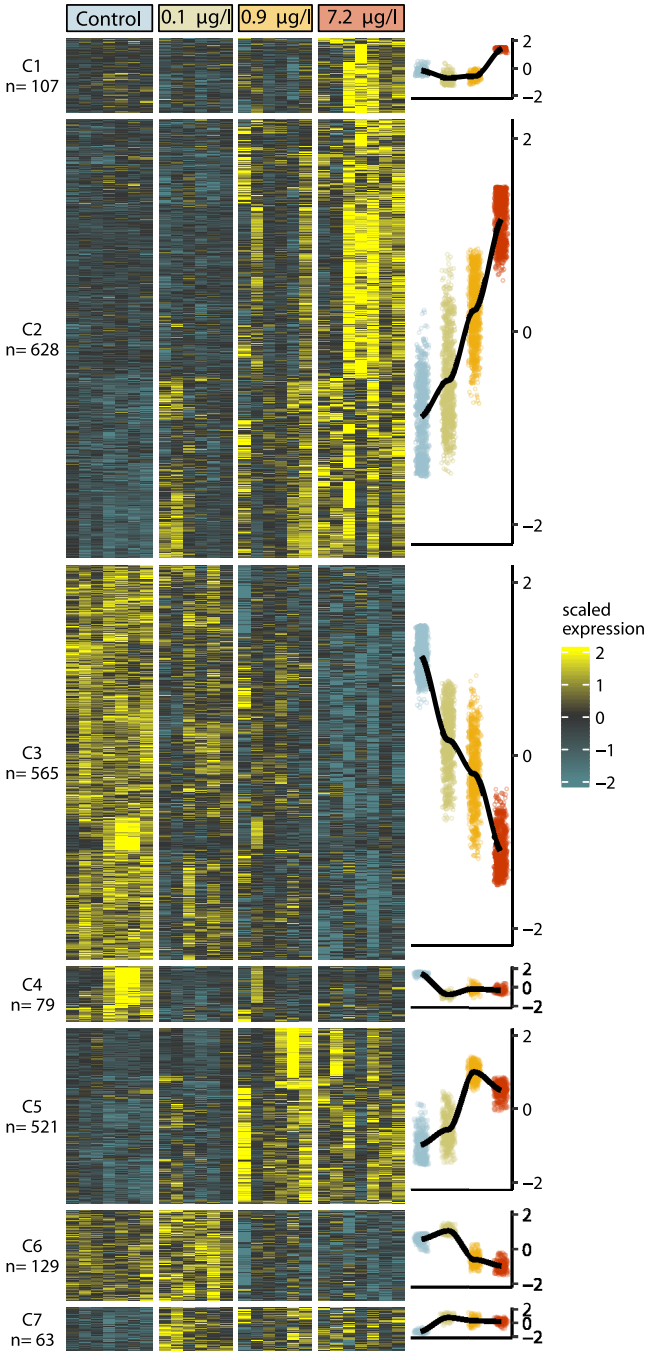

Figure 5. 6PPD-quinone elicited strong dose-dependent modifications in gene expression. Heatmap of the 7 DEG clusters identified by likelihood ratio testing and DIANA hierarchical clustering. *N* represents the number of genes in each gene cluster. Right panel shows the LOESS model fit of scaled gene expression (*y*-axis) with increasing concentration (*x*-axis).

BBB integrity. Our molecular data overwhelmingly indicated that exposure to 6PPD-quinone led to dysregulation of transcripts encoding endothelial barrier integrity and hematological pathways at both AJs and TJs, with the bulk of these changes supporting mechanisms of increased endothelial permeability.

Tight junctions are composed of transmembrane adhesive proteins, including junctional adhesion molecules (JAMs), occludin, and claudins that interact with intracellular zona occludin proteins (*zo-1*, *zo-2*, and *zo-3*) to connect adhesion molecules to the actin cytoskeleton.[49] Genes encoding adhesion molecules *jamc* and occludin were significantly downregulated and intracellular *zo-1* and *zo-2* were significantly upregulated in 6PPD-quinone-exposed embryos (Figure 6C). *In vitro* knockdown of either occludin or JAM alone is sufficient to enhance endothelial permeability.[50,51] Further, we observed significant dysregulation of prominent mediators of BBB permeability at tight junctions that may have led to the decreased expression of TJ adhesive molecules.[49] Transcription of inflammatory mediators, including vascular endothelial growth factor c (*vegfc*), thrombin (*f2*), and proinflammatory molecules interleukin 1 β (*il1β*) and tumor necrosis factor α (*tnfα*) were altered (Figure 6A). Pathway enrichment was observed for two other molecules with well-documented effects on BBB tight junction permeability, interferon γ (*ifnγ*), and transforming growth factor β (*tgfβ*, Figure 6B and Table S2). DEGs from the IFNγ pathway were significantly skewed toward increased expression ($p < 0.05$, Fisher's exact test) that implies pathway activation, which mediates endothelial hyperpermeability by altering cell morphology and rearrangement of the actin cytoskeleton.[52]

VEGF and proinflammatory factors TNFα and thrombin also act at adherens junctions to increase endothelial permeability through serine/threonine kinase-dependent mechanisms[53,54] that lead to phosphorylation and internalization of VE-cadherin, the primary transmembrane adhesion molecule controlling vascular permeability of endothelial AJs. In addition to dysregulation of all three inflammatory mediators, VE-cadherin expression decreased in a dose-dependent manner ($p = 0.07$, Figure 6D), and the transmembrane receptor protein serine/threonine kinase signaling pathway (GO:0007178) was significantly enriched in exposed fish with 40 DEGs (Figure 7A). Extracellular matrix organization was the most significantly enriched gene ontology category, further indicating disruptions in cell−cell contacts (Figure 7A). Hematological-related pathways including coagulation and hemostasis were also affected. Moreover, hematological disruptions were significantly associated with transcripts altered at all three 6PPD-quinone concentrations (DEG clusters 4 and 7, Figure 5), suggesting that substantial effects on vascular permeability may occur after brief exposure and in the absence of any mortality (Fisher's exact test, $p \leq 0.05$, Figure 7A).

Our results strongly implicate increased vascular permeability as a significant effect of 6PPD-quinone in coho salmon. Capillary leak syndrome (CLS) describes manifestations of increased capillary permeability and has primarily been studied in humans with sepsis and Clarkson's disease and with respect to adverse reactions to anticancer drugs.[55,56] In severe cases of CLS, rapid extravasation of plasma into surrounding tissues and loss of blood volume can lead to hypovolemic shock and subsequent ischemia-induced organ failure resulting in death.[57] Symptoms experienced during severe instances of CLS are similar to URMS in several ways. For example, coho salmon in late-stage URMS experience thickening of the blood and increased hemoconcentration of 20−25% that is comparable to fatal instances of CLS in patients with Clarkson's disease.[25,58] Disruptions of the BBB via capillary leak can lead to cerebral edema and impaired motor function and cognition, which may be paralleled by loss of equilibrium, sideways swimming, and spiraling in coho displaying late stages of URMS.[22,59]

https://doi.org/10.1021/acs.est.3c01040
Environ. Sci. Technol. 2023, 57, 10940−10950

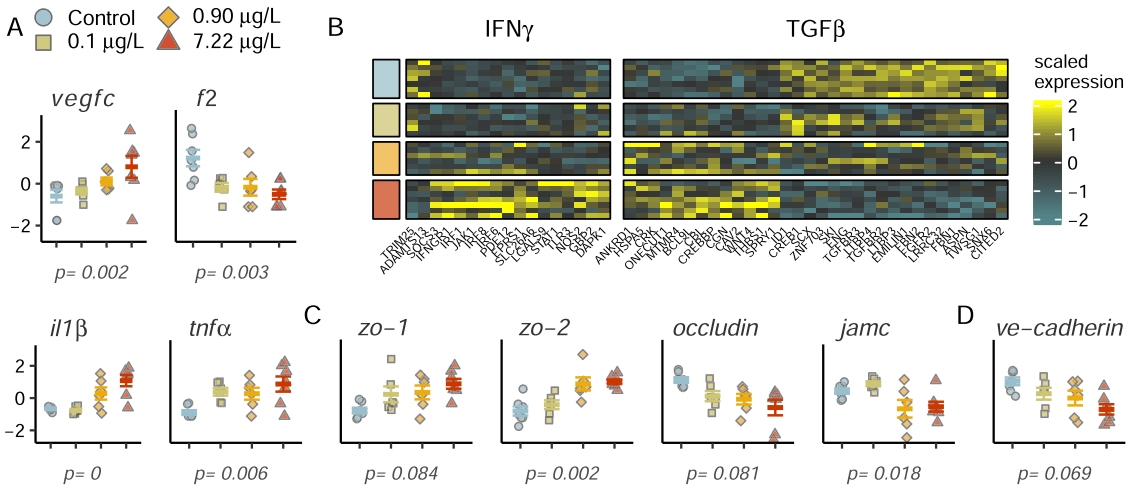

Figure 6. 6PPD-quinone altered expression of mediators and genes involved in endothelial permeability. (A) Expression of permeability mediators vascular endothelial growth factor c (*vegfc*), thrombin (*f2*), interleukin 1 β (*il1β*), and tumor necrosis factor α (*tnfα*). *Y*-axis displays the gene expression *z*-score. (B) Gene ontology enrichment of endothelial permeability mediators interferon γ (IFNγ) and transforming growth factor β (TGFβ). Treatment is indicated on the left side, with colors corresponding to the legend in panel (A). (C) Altered expression of critical components of tight junctions zona occludin (*zo-1* and *zo-2*), occludin, and junction adhesion molecule c (*jamc*). (D) Expression of VE-cadherin, the primary transmembrane protein at adherens junctions. Displayed *p*-values were obtained from likelihood ratio testing in DESeq2.

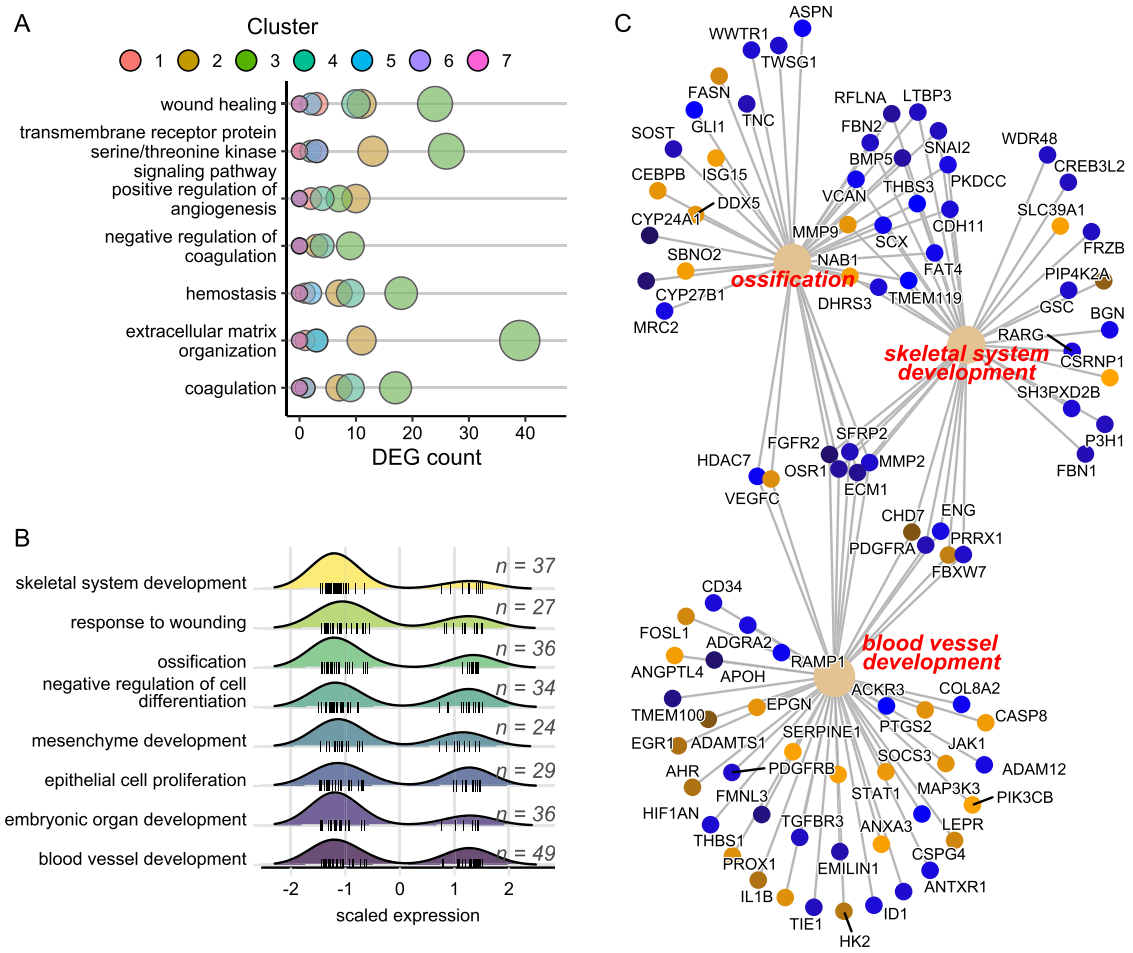

Figure 7. Gene ontology enrichment of hematological and developmental-related pathways. (A) Enrichment of hematological and extracellular organization pathways using the full dataset of DEGs. (B) Density plot of scaled gene expression for DEGs with strong dose-dependent changes (clusters 2 and 3) belonging to development and cell proliferation gene ontologies, with n representing the number of DEGs in each pathway. (C) Linkage network of DEGs in clusters 2 and 3 belonging to the indicated categories. Each node represents the specified DEG, color coded as downregulated (blue, cluster 3) or upregulated (orange, cluster 2) with increasing 6PPD-quinone concentration.

https://doi.org/10.1021/acs.est.3c01040
Environ. Sci. Technol. 2023, 57, 10940−10950

Importantly, induction of inflammatory molecules that were altered by 6PPD-quinone is frequently cited as the driver of CLS as a side effect of anticancer drugs[60] that lead to the loss of surface expression of VE-cadherin in endothelial cells,[61] including *il1β* that was the most significantly altered transcript in this study. Thus, induction of inflammatory responses by 6PPD-quinone in coho salmon presents a potential mechanism promoting endothelial permeability and downstream biological effects. Induction of apoptotic pathways and endothelial cell death are also frequently associated with CLS; however, we did not observe molecular indications of apoptosis induction. Similarly, mitochondrial dysfunction can lead to overproduction of reactive oxygen species (ROS) that are also known modulators of vascular permeability,[62] and mitochondrial dysfunction has also been implicated as a proposed route of 6PPD-quinone toxicity using rainbow trout and coho salmon *in vitro* models.[63,64] However, we did not observe molecular signatures indicating the presence of mitochondrial dysfunction.

We then performed independent pathway analyses on DEG clusters 2 and 3 that contained the majority of the DEGs (1193, 65%), which indicated progressively perturbed expression with increasing concentration of 6PPD-quinone. We removed 401 DEGs that lacked sufficient mapping to human annotations and then assessed gene ontology enrichment analysis with the remaining 792 genes using the corresponding human IDs. Results overwhelmingly supported disruptions in development (blood vessel, skeletal system, mesenchyme, connective tissue, muscle tissue, embryonic organ, heart, face, cartilage), cell differentiation (epithelial cells, osteoblasts), and cell proliferation (epithelial, hepatocytes) (Figure 7B and Table S3). Impacts on developmental pathways were heavily skewed toward DEG cluster 3 showing downregulated expression, despite an approximately equal number of up and down DEGs in the analysis (Figure 7B). Minimal overlap in genes innervating blood vessel development, skeletal system development, and ossification indicated that effects represent a broad organismal response not limited to a core set of shared genes among pathways (Figure 7C). Persistent downregulation of developmental pathways provides a likely mechanism for reductions in total length and eye area in exposed embryos (Figure 4).

In summary, stormwater containing the car tire transformation product 6PPD-quinone is considered to be responsible for prespawn mortality in PNW waterways and will likely have long-term implications for coho salmon populations that transit urban areas in the PNW. Our data suggests that the embryonic chorion of coho salmon embryos provided effective protection from 6PPD-quinone-induced mortality at low concentrations. However, our data implicates that fry and smolt mortality are likely significant factors in population declines of an ESA-listed species. As urbanization and nonpoint source pollution continue to increase globally, our identification of the mechanisms of 6PPD-quinone effects is an important step in understanding the ways in which PPDs exert toxicity. Capillary leak and disruptions of the BBB may be a key event in 6PDD-quinone-induced mortality, and further refinements of the mechanism of action will provide crucial insights into the substantial variability in 6PPD-quinone-induced mortality in salmonids. One critically important question evoked by this study is the potential for 6PPD-quinone bioaccumulation that would further increase concerns for repeated exposures during freshwater residence, as multiple stormwater runoff events are a regular occurrence for coho salmon in the PNW.

■ ASSOCIATED CONTENT

Data Availability Statement

All data underlying the conclusions of this manuscript are freely available online. Raw RNA sequencing reads are deposited at the NCBI Sequence Read Archive, Bioproject PRJNA867720. All other data and all coding scripts used in analyses (RNASeq, statistics) are available on Github at https://github.com/jbg03/coho_embryos_6PPD-quinone.

Supporting Information

The Supporting Information is available free of charge at https://pubs.acs.org/doi/10.1021/acs.est.3c01040.

DEGs from RNASeq (Table S1) (TXT)

Gene ontology results (Table S2) (TXT)

Gene ontology results for RNASeq clusters 2 and 3 (Table S3) (TXT)

■ AUTHOR INFORMATION

Corresponding Author

Justin B. Greer − *U.S. Geological Survey, Western Fisheries Research Center, Seattle, Washington 98115, United States;* orcid.org/0000-0001-6660-9976; Phone: (206) 526-2055; Email: jgreer@usgs.gov

Authors

Ellie M. Dalsky − *U.S. Geological Survey, Western Fisheries Research Center, Seattle, Washington 98115, United States;* orcid.org/0000-0001-8299-7198

Rachael F. Lane − *U.S. Geological Survey, Kansas Water Science Center, Lawrence, Kansas 66049, United States;* orcid.org/0000-0001-9202-0612

John D. Hansen − *U.S. Geological Survey, Western Fisheries Research Center, Seattle, Washington 98115, United States*

Complete contact information is available at: https://pubs.acs.org/10.1021/acs.est.3c01040

Author Contributions

J.B.G. and J.D.H. conceived and designed the experiments. J.B.G. and E.M.D. performed the experiments and R.F.L. analyzed water chemistry. J.B.G. analyzed the data. All authors contributed to the writing and editing of the manuscript.

Notes

The authors declare no competing financial interest.

■ ACKNOWLEDGMENTS

The present study was supported by the U.S. Geological Survey, Environmental Health Program, Ecosystems Mission Area, and the U.S. Environmental Protection Agency Puget Sound Geographic Program (Interagency Agreement DW-014-92581001). The authors would like to thank the Issaquah Salmon Hatchery and Yakima Nation Fisheries Hatchery Complex for providing coho salmon embryos for this study. They would also like to thank Holly Clark and Clay Clark for their assistance with sequencing, Crawford Drury and Chris Amemiya for their critical reading and comments on the manuscript, and Prarthana Shankar for assistance creating the experimental design figure. All data underlying the conclusions of this manuscript are available at the U.S. Geological Survey at https://doi.org/10.5066/P9PYKOPH.[65] Any use of trade,

firm, or product names is for descriptive purposes only and does not imply endorsement by the U.S. Government.

REFERENCES

(1) Bradford, M. J.; Irvine, J. R. Land use, fishing, climate change, and the decline of Thompson River, British Columbia, coho salmon. *Can. J. Fish. Aquat. Sci.* **2000**, *57*, 13−16.

(2) Schindler, D. E.; Augerot, X.; Fleishman, E.; Mantua, N. J.; Riddell, B.; Ruckelshaus, M.; Seeb, J.; Webster, M. Climate change, ecosystem impacts, and management for Pacific salmon. *Fisheries* **2008**, *33*, 502−506.

(3) Wainwright, T. C.; Weitkamp, L. A. Effects of climate change on Oregon Coast coho salmon: habitat and life-cycle interactions. *Northwest Sci.* **2013**, *87*, 219−242.

(4) Good, T. P.; Beechie, T. J.; McElhany, P.; McClure, M. M.; Ruckelshaus, M. H. Recovery planning for Endangered Species Act-listed Pacific salmon: using science to inform goals and strategies. *Fisheries* **2007**, *32*, 426−440.

(5) Brown, L. R.; Moyle, P. B.; Yoshiyama, R. M. Historical decline and current status of coho salmon in California. *N. Am. J. Fish. Manage.* **1994**, *14*, 237−261.

(6) Scholz, N. L.; Myers, M. S.; McCarthy, S. G.; Labenia, J. S.; McIntyre, J. K.; Ylitalo, G. M.; Rhodes, L. D.; Laetz, C. A.; Stehr, C. M.; French, B. L.; et al. Recurrent die-offs of adult coho salmon returning to spawn in Puget Sound lowland urban streams. *PLoS One* **2011**, *6*, No. e28013.

(7) Feist, B. E.; Buhle, E. R.; Baldwin, D. H.; Spromberg, J. A.; Damm, S. E.; Davis, J. W.; Scholz, N. L. Roads to ruin: conservation threats to a sentinel species across an urban gradient. *Ecol. Appl.* **2017**, *27*, 2382−2396.

(8) Spromberg, J. A.; Scholz, N. L. Estimating the future decline of wild coho salmon populations resulting from early spawner die-offs in urbanizing watersheds of the Pacific Northwest, USA. *Integr. Environ. Assess. Manage.* **2011**, *7*, 648−656.

(9) Tian, Z.; Zhao, H.; Peter, K. T.; Gonzalez, M.; Wetzel, J.; Wu, C.; Hu, X.; Prat, J.; Mudrock, E.; Hettinger, R. A ubiquitous tire rubber−derived chemical induces acute mortality in coho salmon. *Science* **2021**, *371*, 185−189.

(10) Kruger, R. H.; Boissière, C.; Klein-Hartwig, K.; Kretzschmar, H.-J. New phenylenediamine antiozonants for commodities based on natural and synthetic rubber. *Food Addit. Contam.* **2005**, *22*, 968−974.

(11) Johannessen, C.; Helm, P.; Lashuk, B.; Yargeau, V.; Metcalfe, C. D. The tire wear compounds 6PPD-quinone and 1, 3-diphenylguanidine in an urban watershed. *Arch. Environ. Contam. Toxicol.* **2022**, *82*, 171−179.

(12) Rauert, C.; Charlton, N.; Okoffo, E. D.; Stanton, R. S.; Agua, A. R.; Pirrung, M. C.; Thomas, K. V. Concentrations of Tire Additive Chemicals and Tire Road Wear Particles in an Australian Urban Tributary. *Environ. Sci. Technol.* **2022**, *56*, 2421−2431.

(13) Challis, J. K.; Popick, H.; Prajapati, S.; Harder, P.; Giesy, J. P.; McPhedran, K.; Brinkmann, M. Occurrences of tire rubber-derived contaminants in cold-climate urban runoff. *Environ. Sci. Technol. Lett.* **2021**, *8*, 961−967.

(14) Seiwert, B.; Nihemaiti, M.; Troussier, M.; Weyrauch, S.; Reemtsma, T. Abiotic oxidative transformation of 6-PPD and 6-PPD quinone from tires and occurrence of their products in snow from urban roads and in municipal wastewater. *Water Res.* **2022**, *212*, No. 118122.

(15) Tian, Z.; Gonzalez, M.; Rideout, C. A.; Zhao, H. N.; Hu, X.; Wetzel, J.; Mudrock, E.; James, C. A.; McIntyre, J. K.; Kolodziej, E. P. 6PPD-quinone: Revised toxicity assessment and quantification with a commercial standard. *Environ. Sci. Technol. Lett.* **2022**, *9*, 140−146.

(16) Zeng, L.; Li, Y.; Sun, Y.; Liu, L.-Y.; Shen, M.; Du, B. Widespread Occurrence and Transport of p-Phenylenediamines and Their Quinones in Sediments across Urban Rivers, Estuaries, Coasts, and Deep-Sea Regions. *Environ. Sci. Technol.* **2023**, *57*, 2393−2403.

(17) Cao, G.; Wang, W.; Zhang, J.; Wu, P.; Zhao, X.; Yang, Z.; Hu, D.; Cai, Z. New Evidence of Rubber-Derived Quinones in Water, Air, and Soil. *Environ. Sci. Technol.* **2022**, *56*, 4142−4150.

(18) Huang, W.; Shi, Y.; Huang, J.; Deng, C.; Tang, S.; Liu, X.; Chen, D. Occurrence of substituted p-phenylenediamine antioxidants in dusts. *Environ. Sci. Technol. Lett.* **2021**, *8*, 381−385.

(19) Wu, Y.; Venier, M.; Hites, R. A. Broad exposure of the North American environment to phenolic and amino antioxidants and to ultraviolet filters. *Environ. Sci. Technol.* **2020**, *54*, 9345−9355.

(20) Hiki, K.; Yamamoto, H. Concentration and leachability of N-(1, 3-dimethylbutyl)-N′-phenyl-p-phenylenediamine (6PPD) and its quinone transformation product (6PPD-Q) in road dust collected in Tokyo, Japan. *Environ. Pollut.* **2022**, *302*, No. 119082.

(21) Du, B.; Liang, B.; Li, Y.; Shen, M.; Liu, L.-Y.; Zeng, L. First Report on the Occurrence of N-(1, 3-Dimethylbutyl)-N′-phenyl-p-phenylenediamine (6PPD) and 6PPD-Quinone as Pervasive Pollutants in Human Urine from South China. *Environ. Sci. Technol. Lett.* **2022**, *9*, 1056−1062.

(22) Chow, M. I.; Lundin, J. I.; Mitchell, C. J.; Davis, J. W.; Young, G.; Scholz, N. L.; McIntyre, J. K. An urban stormwater runoff mortality syndrome in juvenile coho salmon. *Aquat. Toxicol.* **2019**, *214*, No. 105231.

(23) McIntyre, J. K.; Lundin, J. I.; Cameron, J. R.; Chow, M. I.; Davis, J. W.; Incardona, J. P.; Scholz, N. L. Interspecies variation in the susceptibility of adult Pacific salmon to toxic urban stormwater runoff. *Environ. Pollut.* **2018**, *238*, 196−203.

(24) French, B. F.; Baldwin, D. H.; Cameron, J.; Prat, J.; King, K.; Davis, J. W.; McIntyre, J. K.; Scholz, N. L. Urban Roadway Runoff Is Lethal to Juvenile Coho, Steelhead, and Chinook Salmonids, But Not Congeneric Sockeye. *Environ. Sci. Technol. Lett.* **2022**, *9*, 733−738.

(25) Blair, S. I.; Barlow, C. H.; McIntyre, J. K. Acute cerebrovascular effects in juvenile coho salmon exposed to roadway runoff. *Can. J. Fish. Aquat. Sci.* **2021**, *78*, 103−109.

(26) Brinkmann, M.; Montgomery, D.; Selinger, S.; Miller, J. G. P.; Stock, E.; Alcaraz, A. J.; Challis, J. K.; Weber, L.; Janz, D.; Hecker, M.; Wiseman, S. Acute toxicity of the tire rubber-derived chemical 6ppd-quinone to four fishes of commercial, cultural, and ecological importance. *Environ. Sci. Technol. Lett.* **2022**, *9*, 333−338.

(27) Hiki, K.; Asahina, K.; Kato, K.; Yamagishi, T.; Omagari, R.; Iwasaki, Y.; Watanabe, H.; Yamamoto, H. Acute toxicity of a tire rubber-derived chemical, 6PPD quinone, to freshwater fish and crustacean species. *Environ. Sci. Technol. Lett.* **2021**, *8*, 779−784.

(28) Foldvik, A.; Kryuchkov, F.; Sandodden, R.; Uhlig, S. Acute toxicity testing of the tire rubber-derived chemical 6PPD-quinone on Atlantic salmon (*Salmo salar*) and brown trout (*Salmo trutta*). *Environ. Toxicol. Chem.* **2022**, *41*, 3041−3045.

(29) Hiki, K.; Yamamoto, H. The Tire-Derived Chemical 6PPD-quinone Is Lethally Toxic to the White-Spotted Char *Salvelinus leucomaenis* pluvius but Not to Two Other Salmonid Species. *Environ. Sci. Technol. Lett.* **2022**, *9*, 1050−1055.

(30) Bolger, A. M.; Lohse, M.; Usadel, B. Trimmomatic: a flexible trimmer for Illumina sequence data. *Bioinformatics* **2014**, *30*, 2114−2120.

(31) Andrews, S. FastQC: a quality control tool for high throughput sequence data. http://www.bioinformatics.babraham.ac.uk/projects/fastqc.

(32) Patro, R.; Duggal, G.; Love, M. I.; Irizarry, R. A.; Kingsford, C. Salmon provides fast and bias-aware quantification of transcript expression. *Nat. Methods* **2017**, *14*, 417−419.

(33) Love, M. I.; Huber, W.; Anders, S. Moderated estimation of fold change and dispersion for RNA-seq data with DESeq. 2. *Genome Biol.* **2014**, *15*, No. 550.

(34) Pantano, L. *DEGreport: Report of DEG analysis*, 2017.

(35) Gu, Z.; Eils, R.; Schlesner, M. Complex heatmaps reveal patterns and correlations in multidimensional genomic data. *Bioinformatics* **2016**, *32*, 2847−2849.

(36) Yu, G.; Wang, L.-G.; Han, Y.; He, Q.-Y. clusterProfiler: an R package for comparing biological themes among gene clusters. *OMICS: J. Integr. Biol.* **2012**, *16*, 284−287.

(37) Peter, K. T.; Hou, F.; Tian, Z.; Wu, C.; Goehring, M.; Liu, F.; Kolodziej, E. P. More than a first flush: Urban creek storm

hydrographs demonstrate broad contaminant pollutographs. *Environ. Sci. Technol.* **2020**, *54*, 6152−6165.
(38) Johnson, S. C.; Chapman, G. A.; Stevens, D. G. Relationships between temperature units and sensitivity to handling for coho salmon and rainbow trout embryos. *Prog. Fish-Cult.* **1989**, *51*, 61−68.
(39) Henn, K.; Braunbeck, T. Dechorionation as a tool to improve the fish embryo toxicity test (FET) with the zebrafish (*Danio rerio*). *Comp. Biochem. Physiol., Part C: Toxicol. Pharmacol.* **2011**, *153*, 91−98.
(40) Braunbeck, T.; Böttcher, M.; Hollert, H.; Kosmehl, T.; Lammer, E.; Leist, E.; Rudolf, M.; Seitz, N. Towards an alternative for the acute fish LC50 test in chemical assessment: the fish embryo toxicity test goes multi-species-an update. *ALTEX-Altern. Anim. Exp.* **2005**, *22*, 87−102.
(41) Fent, K.; Weisbrod, C. J.; Wirth-Heller, A.; Pieles, U. Assessment of uptake and toxicity of fluorescent silica nanoparticles in zebrafish (*Danio rerio*) early life stages. *Aquat. Toxicol.* **2010**, *100*, 218−228.
(42) Pelka, K. E.; Henn, K.; Keck, A.; Sapel, B.; Braunbeck, T. Size does matter−Determination of the critical molecular size for the uptake of chemicals across the chorion of zebrafish (*Danio rerio*) embryos. *Aquat. Toxicol.* **2017**, *185*, 1−10.
(43) Manahan, C. Assessment of potential hazards of 6PPD and alternatives. https://www.ezview.wa.gov/Portals/_1962/Documents/6ppd/6PPD%20Alternatives%20Technical%20Memo.pdf.
(44) Chittenden, C. M.; Melnychuk, M. C.; Welch, D. W.; McKinley, R. S. An investigation into the poor survival of an endangered coho salmon population. *PLoS One* **2010**, *5*, No. e10869.
(45) McIntyre, J. K.; Prat, J.; Cameron, J.; Wetzel, J.; Mudrock, E.; Peter, K. T.; Tian, Z.; Mackenzie, C.; Lundin, J.; Stark, J. D.; et al. Treading water: tire wear particle leachate recreates an urban runoff mortality syndrome in coho but not chum salmon. *Environ. Sci. Technol.* **2021**, *55*, 11767−11774.
(46) Brooks, T. A.; Hawkins, B. T.; Huber, J. D.; Egleton, R. D.; Davis, T. P. Chronic inflammatory pain leads to increased blood-brain barrier permeability and tight junction protein alterations. *Am. J. Physiol.: Heart Circ. Physiol.* **2005**, *289*, H738−H743.
(47) Hawkins, B. T.; Davis, T. P. The blood-brain barrier/neurovascular unit in health and disease. *Pharmacol. Rev.* **2005**, *57*, 173−185.
(48) Komarova, Y. A.; Kruse, K.; Mehta, D.; Malik, A. B. Protein interactions at endothelial junctions and signaling mechanisms regulating endothelial permeability. *Circ. Res.* **2017**, *120*, 179−206.
(49) Cerutti, C.; Ridley, A. J. Endothelial cell-cell adhesion and signaling. *Exp. Cell Res.* **2017**, *358*, 31−38.
(50) Laukoetter, M. G.; Nava, P.; Lee, W. Y.; Severson, E. A.; Capaldo, C. T.; Babbin, B. A.; Williams, I. R.; Koval, M.; Peatman, E.; Campbell, J. A.; et al. JAM-A regulates permeability and inflammation in the intestine in vivo. *J. Exp. Med.* **2007**, *204*, 3067−3076.
(51) Al-Sadi, R.; Khatib, K.; Guo, S.; Ye, D.; Youssef, M.; Ma, T. Occludin regulates macromolecule flux across the intestinal epithelial tight junction barrier. *Am. J. Physiol.: Gastrointest. Liver Physiol.* **2011**, *300*, G1054−G1064.
(52) Ng, C. T.; Fong, L. Y.; Sulaiman, M. R.; Moklas, M. A. M.; Yong, Y. K.; Hakim, M. N.; Ahmad, Z. Interferon-gamma increases endothelial permeability by causing activation of p38 MAP kinase and actin cytoskeleton alteration. *J. Interferon Cytokine Res.* **2015**, *35*, 513−522.
(53) Weis, S.; Shintani, S.; Weber, A.; Kirchmair, R.; Wood, M.; Cravens, A.; McSharry, H.; Iwakura, A.; Yoon, Y.-s.; Himes, N.; et al. Src blockade stabilizes a Flk/cadherin complex, reducing edema and tissue injury following myocardial infarction. *J. Clin. Invest.* **2004**, *113*, 885−894.
(54) Jaken, S. Protein kinase C isozymes and substrates. *Curr. Opin. Cell Biol.* **1996**, *8*, 168−173.
(55) Jeong, G. H.; Lee, K. H.; Lee, I. R.; Oh, J. H.; Kim, D. W.; Shin, J. W.; Kronbichler, A.; Eisenhut, M.; van der Vliet, H. J.; Abdel-Rahman, O.; et al. Incidence of capillary leak syndrome as an adverse effect of drugs in cancer patients: a systematic review and meta-analysis. *J. Clin. Med.* **2019**, *8*, No. 143.
(56) Siddall, E.; Khatri, M.; Radhakrishnan, J. Capillary leak syndrome: etiologies, pathophysiology, and management. *Kidney Int.* **2017**, *92*, 37−46.
(57) Druey, K. M.; Greipp, P. R. Narrative review: the systemic capillary leak syndrome. *Ann. Intern. Med.* **2010**, *153*, 90−98.
(58) Kapoor, P.; Greipp, P. T.; Schaefer, E. W.; Mandrekar, S. J.; Kamal, A. H.; Gonzalez-Paz, N. C.; Kumar, S.; Greipp, P. R. Idiopathic systemic capillary leak syndrome (Clarkson's disease): the Mayo clinic experience. *Mayo Clin. Proc.* **2010**, *85*, 905−912.
(59) Stamatovic, S. M.; Johnson, A. M.; Keep, R. F.; Andjelkovic, A. V. Junctional proteins of the blood-brain barrier: New insights into function and dysfunction. *Tissue Barriers* **2016**, *4*, No. e1154641.
(60) Izzedine, H.; Mathian, A.; Amoura, Z.; Ng, J. H.; Jhaveri, K. D. Anticancer Drugs-induced Capillary Leak Syndrome. *Kidney Int. Rep.* **2022**, 945−953.
(61) Puhlmann, M.; Weinreich, D. M.; Farma, J. M.; Carroll, N. M.; Turner, E. M.; Alexander, H. R. Interleukin-1β induced vascular permeability is dependent on induction of endothelial tissue factor (TF) activity. *J. Transl. Med.* **2005**, *3*, No. 37.
(62) He, P.; Talukder, M. A. H.; Gao, F. Oxidative stress and microvessel barrier dysfunction. *Front. Physiol.* **2020**, *11*, No. 472.
(63) Mahoney, H.; da Silva Junior, F. C.; Roberts, C.; Schultz, M.; Ji, X.; Alcaraz, A. J.; Montgomery, D.; Selinger, S.; Challis, J. K.; Giesy, J. P.; et al. Exposure to the tire rubber-derived contaminant 6PPD-Quinone causes mitochondrial dysfunction in vitro. *Environ. Sci. Technol. Lett.* **2022**, *9*, 765−771.
(64) Greer, J. B.; Dalsky, E. M.; Lane, R. F.; Hansen, J. D. Establishing an In Vitro Model to Assess the Toxicity of 6PPD-Quinone and Other Tire Wear Transformation Products. *Environ. Sci. Technol. Lett.* **2023**, *10*, 533−537.
(65) Greer, J. B. *Mortality, morphology, and water chemistry for 6PPD-quinone exposed coho embryos*, U.S. Geological Survey data release, 2023.

https://doi.org/10.1021/acs.est.3c01040
Environ. Sci. Technol. 2023, 57, 10940−10950